JOURNAL OF SOLID STATE CHEMISTRY 38, 239–245 (1981)

Neutron Powder Diffraction on α-Tl_4CrI_6 and β-Tl_4CrI_6

H. W. ZANDBERGEN

Gorlaeus Laboratories, University of Leiden, P.O. Box 9502, 2300 RA Leiden, The Netherlands

Received September 22, 1980; in final form December 4, 1980

α-Tl_4CrI_6 (a = 9.132(1), c = 9.667(1) Å, Z = 2, $P4/mnc$ at 293 K) adopts a distorted Tl_4HgBr_6 structure. In α-Tl_4CrI_6 there occurs a random distribution of Jahn–Teller distorted octahedra which are elongated perpendicular to the c axis. Between 77 and 4.2 K a phase transition occurs. In β-Tl_4CrI_6 (a = 12.941(3), b = 12.596(3), c = 9.602(2) Å, Z = 4, $Cccm$ at 4.2 K) the directions of elongation of the octahedra are ordered. The structure is very much related to that of α-Tl_4CrI_6. A three-dimensional magnetic ordering takes place at 2.7(2) K. The magnetic space group at 1.2 K is $C_I22'2'$. The magnetic moments (3.48(6) μ_B) are parallel to (0 0 1) and have an angle of 41(9)° with the a axis. Four magnetic sublattices are present, forming two independent magnetic lattices which have no interaction due to the antiparallel ordering.

Introduction

In an earlier paper (*1*) the determination of the crystal structure of α-Tl_4CrI_6 by means of X-ray single-crystal diffraction was reported. Strong evidence was found for the occurrence of Jahn–Teller deformed octahedra in this phase. The octahedra are elongated perpendicular to the c axis; the direction of elongation is distributed randomly over the two possibilities. Jouini *et al.* (*2*) reported also the structure of α-Tl_4CrI_6; however they did not account for the Jahn–Teller effect. Due to a coupling of the Jahn–Teller deformations a complete ordering of the elongation directions is expected to occur at lower temperature. In this paper the crystal structure of β-Tl_4CrI_6 and its magnetic structure at 1.2 K is reported together with magnetic measurements on a powder of Tl_4CrI_6.

Experimental

The samples of Tl_4CrI_6 used for neutron diffraction and magnetic measurements were prepared by melting and annealing for 2 weeks at 350°C a stoichiometric mixture of the binary compounds. The binary compounds were purified by distillation (TlI) or sublimation (CrI_2). Since Tl_4CrI_6 is very hygroscopic, all manipulations were carried out in a dry glovebox in argon.

Neutron powder diffraction was done at 293, 77, 4.2, and 1.2 K at the HFR reactor at Petten (The Netherlands) using λ = 2.5783(1) Å with 30′ collimation in the angular range $4° < 2\theta < 140°$. No absorption correction was applied. The coherent scattering lengths (*3*) used are b(Tl) = 0.89, b(Cr) = 0.352, and b(I) = 0.53, all in units of 10^{-12} cm. Magnetic form factors were taken from Watson and Freeman (*4*). For

0022-4596/81/080239-07$02.00/0

the refinements, the profile refinement method of Rietveld (5) was used.

Magnetic measurements were carried out by means of a vibrating sample magnetometer with fields up to 56 kOe (6).

Refinements with the Neutron Diffraction Data

α-Tl_4CrI_6 (293 K)

The refinement was started with the positions of α-Tl_4CrI_6 from (1). To account for the random distribution of elongated octahedra I(2) is distributed over two equally occupied positions. Refinements in space group $P4/mnc$ led to convergence at

$$R(\text{total}) = \sum_i |I_i(\text{obs}) - (1/c)I_i(\text{calc})| / \sum_i I_i(\text{obs}) = 0.037$$

and

$$R(\text{profile}) = \left\{ \sum_j w_j [y_j(\text{obs}) - (1/c)y_j(\text{calc})]^2 / \sum_j w_j y_j(\text{calc})^2 \right\}^{1/2} = 0.096$$

with a nondivided I(2) ion and R(total) = 0.035 and R(profile) = 0.094 with a divided I(2) ion. In the refinement with the divided I(2) ion the shifts of the two parts were negatively coupled. The results of these refinements are given in Table I.

α-Tl_4CrI_6 (77 K)

The diffraction diagram recorded at liquid nitrogen temperature is almost identical to that of 293 K, showing the phase transition α-$Tl_4CrI_6 \rightarrow \beta$-$Tl_4CrI_6$ to take place below this temperature. Refinements similar to the ones of the recording at 293 K resulted in R(total) = 0.059 and R(profile) = 0.092 and R(total) = 0.052 and R(profile) = 0.085 for the refinements with a nondivided and a divided I(2) ion, respectively. The results are given in Table I. The observed and calculated profiles are depicted in Fig. 1A.

TABLE I

POSITIONAL AND ISOTROPIC THERMAL PARAMETERS (b) OF α-Tl_4CrI_6 AT 293 K AND 77 K AND OF β-Tl_4CrI_6 AT 4.2 AND 1.2 K[a]

	x	y	z	b
		293 K		
		a = 9.132(1), c = 9.661(1) Å		
Tl	0.1449(2)	0.3551(2)	0.25	3.4(1)
Cr	0	0	0	2.0(4)
I(1)	0	0	0.2839(7)	1.7(2)
I(2)	0.3049(4)	0.1371(6)	0	2.6(1)
I(2a)	0.3219(17)	0.1436(19)	0	1.9(2)
I(2b)	0.2879(17)	0.1307(19)	0	
		77K		
		a = 9.013(1), b = 9.580(1) Å		
Tl	0.1445(2)	0.3555(2)	0.25	1.5(1)
Cr	0	0	0	0.6(4)
I(1)	0	0	0.2871(6)	0.3(2)
I(2)	0.3032(4)	0.1390(5)	0	0.8(1)
I(2a)	0.3233(11)	0.1517(11)	0	−0.1(1)
I(2b)	0.2831(11)	0.1263(11)	0	
		4.2 K		
		a = 12.941(3), b = 12.596(3), c = 9.602(2) Å, b(overall) = 0.6(1) Å²		
Tl(1)	0.1406(5)	0	0.25	
Tl(2)	0	0.3524(5)	0.25	
Cr	0.25	0.25	0	
I(1)	0.25	0.25	0.2896(12)	
I(2)	0.3268(9)	0.0345(9)	0	
I(3)	0.0191(11)	0.1692(10)	0	
		1.2 K		
		a = 12.927(3), b = 12.584(3), c = 9.593(2) Å, b(overall) = 0.6(1) Å²		
Tl(1)	0.1414(6)	0	0.25	
Tl(2)	0	0.3522(6)	0.25	
Cr	0.25	0.25	0	
I(1)	0.25	0.25	0.2901(13)	
I(2)	0.3257(9)	0.0348(9)	0	
I(3)	0.0189(12)	0.1692(10)	0	

Magnetic moment: μ_x = 2.5(5) μ_y = 2.1(6)
μ_{TOTAL} = 3.48(6) μ_B

[a] I(2a) and I(2b) represent the divided parts of I(2) as discussed in the text. The positions of the other ions are equal for both refinements.

β-Tl_4CrI_6 (4.2 K)

The diffraction diagram recorded at 4.2 K

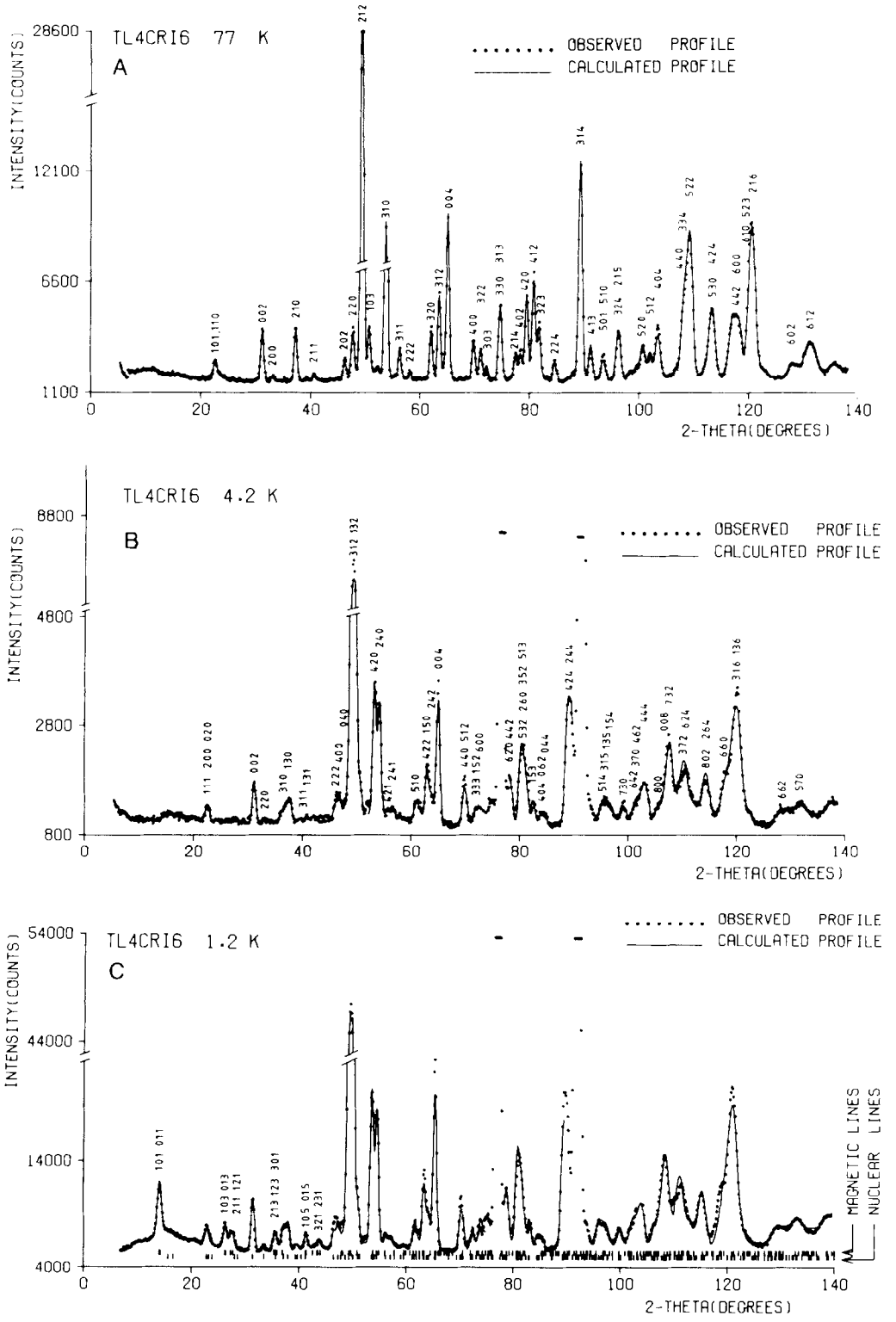

FIG. 1. The observed and calculated profiles of (A) α-Tl_4CrI_6 at 77 K and β-Tl_4CrI_6 at (B) 4.2 and (C) 1.2 K. The indices of most of the reflections are given.

shows several peaks to be split up. The peaks could be indexed with a C-centered orthorhombic unit cell with axes of about $a2^{1/2}$, $a2^{1/2}$, c; a and c being the axes of the tetragonal unit cell of α-Tl_4CrI_6. The Jahn–Teller deformation of the high-temperature phase suggests the space group $Cccm$. Besides refinement in this space group refinement was also done in the space groups $Ccc2$ (R(profile) = 0.122) and $C222$ (R(profile) = 0.123), yielding R values which are not significantly lower with respect to those of the refinement in space group $Cccm$. It is concluded that the space group of β-Tl_4CrI_6 is $Cccm$ also because the distortion of the octahedra is similar to the distortion in α-Tl_4CrI_6. The final R values are R(total) = 0.049 and R(profile) = 0.124. The results of the refinement are shown in Fig. 1B and listed in Table I.

β-Tl_4CrI_6 (1.2 K)

The diffraction pattern recorded at 1.2 K contains a number of magnetic reflections, which can be indexed with an a, b, $2c$ unit cell, a, b, and c being the axes of the nuclear unit cell of β-Tl_4CrI_6.

No magnetic reflections with $h + k = 2n$ occur, suggesting the magnetic space lattice type to be C_I. This yields the magnetic space groups C_I222 and $C_I22'2'$ (*7*) with the magnetic moments oriented perpendicular and parallel to the (0 0 1) plane, respectively, due to the symmetry. Both models were refined. The R values and the fits showed the magnetic movements to be parallel to the (0 0 1) plane with an angle of 41(9)° with the a axis. The standard deviation of the angle is high because the a and the b axis are almost equal. The final R values are R(profile) = 0.117 and R(total) = 0.059, which can be divided into a nuclear part, R(nuclear) = 0.057, and a magnetic part, R(magnetic) = 0.078. The observed and calculated profiles are shown in Fig. 1C and the results of the refinements are given in Table I.

Magnetic Measurements

On a powder sample of Tl_4CrI_6 M vs H measurements at 2 K up to 56 kOe and χ vs T measurements in the temperature range 2–100 K were carried out. No field dependence of dM/dH was found. The $1/\chi$ vs T of Tl_4CrI_6 is depicted in Fig. 2. The three-dimensional transition temperature is determined to be 2.7(2) K for β-Tl_4CrI_6, at which temperatures $d\chi/dT$ is maximal. From the linear part of $1/\chi$ vs T, θ, and μ(eff) were found to be $-7(2)$ K and 4.5(2) μ_B. A deviation from the linear temperature dependence of $1/\chi$ is found to start at about 6 K.

Discussion

The crystal structure of α-Tl_4CrI_6 is adopted (except for the Jahn–Teller deformation) by many A_4BI_6 compounds with A being In or Tl. Although the K^+ and Rb^+ ions have similar radii, no K_4BI_6 or Rb_4BI_6 compounds exist. The structure of α-Tl_4CrI_6 is probably favored by the In and Tl compounds because of the lone pairs of the In^+ and Tl^+ ions.

Similar to the results obtained for the refinements of the X-ray single-crystal diffraction data (*1*), significantly lower R values for the neutron diffraction recording at 293 and 77 K are obtained for a model with a distribution of the I(2) ions over two equally occupied positions. The effect is greater at 77 K, as expected, since the isotropic thermal parameter, which can partly account for the division of the I ion, is much smaller at this temperature. By this division, elongated octahedra are obtained. The Cr–I distances of both models are listed in Table II. As can be seen from this table the Cr–I distances are similar in α-Tl_4CrI_6 and β-Tl_4CrI_6. X-Ray single-crystal

TABLE II

THE Cr–I DISTANCES IN α-Tl_4CrI_6 AT 293 AND 77 K AND β-Tl_4CrI_6 AT 4.2 AND 1.2 K

	293 K	77 K		4.2 K	1.2 K
Cr–I(1)	2.744(6)	2.750(6) 2×	Cr–I(1)	2.78(1)	2.78(1) 2×
Cr–I(2)	3.053(4)	3.006(4) 4×	Cr–I(2)	2.89(1)	2.89(1) 2×
Cr–I(2a)	3.222(16)	3.219(10)	Cr–I(3)	3.16(1)	3.16(1) 2×
Cr–I(2b)	2.884(16)	2.794(10)			

diffraction on α-Tl_4CrI_6 at 293 K (*1*) resulted in similar and more significant results. X-Ray single-crystal diffraction on α-$CsCrCl_3$ and α-$CsCrI_3$ (*8*) has also given evidence for the existence of elongated octahedra in these phases, which is, furthermore, in accordance with the fact that no difference is observed in the ligand field spectra of $CsCrCl_3$ above or below the phase transition (*8*, *9*). It is concluded that in α-Tl_4CrI_6 elongated octahedra do occur in the high-temperature phase. An oscillation of I(2) between the two positions, with a large probability of finding I(2) at one of these positions, will probably occur. The structure of α-Tl_4CrI_6 is depicted in Fig. 3.

Between 77 and 4.2 K an ordering of the elongated octahedra takes place. Refinements on the diffraction data recorded at 4.2 K showed the space group of β-Tl_4CrI_6 to be *Cccm*. The structure of the low-temperature phase is very similar to the structure of α-Tl_4CrI_6. The only difference is an ordering of the directions of elongation of the octahedra, which results in a difference in the axes *a* and *b*. The structure of β-Tl_4CrI_6 is depicted in Fig. 4.

The magnetic structure of β-Tl_4CrI_6 at 1.2 K is shown in Fig. 5. The magnetic lattice can be divided into four sublattices, $\mathbf{M}_1$, $\mathbf{M}_2$, $\mathbf{M}_3$, and $\mathbf{M}_4$ (see Fig. 6); there is no effective exchange interaction between the Cr^{2+} ions forming the sublattices $\mathbf{M}_1$ and $\mathbf{M}_2$ and the Cr^{2+} ions forming $\mathbf{M}_3$ and $\mathbf{M}_4$. Five types of superexchange interactions between nearest and next nearest neighbor Cr^{2+} ions via two I^- ions exist, as is shown in Fig. 6. The interaction between the sublattices $\mathbf{M}_1$, $\mathbf{M}_2$ and $\mathbf{M}_3$, $\mathbf{M}_4$ will be determined by J_4 and J_5. J_5 has an exchange path via a half-filled *d* orbital of one Cr^{2+} ion and an empty *d* orbital of the other Cr^{2+} ion. Goodenough (*10*) predicts that this yields a

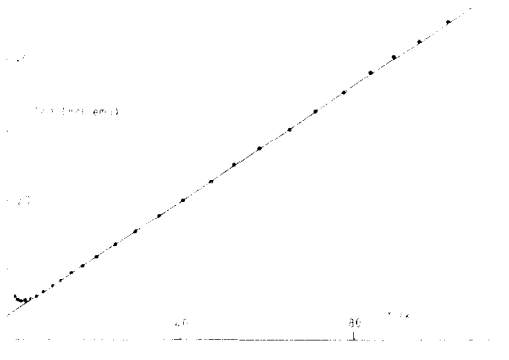

FIG. 2. $1/\chi$ vs T curve of Tl_4CrI_6 measured in a field of 1.1 kOe.

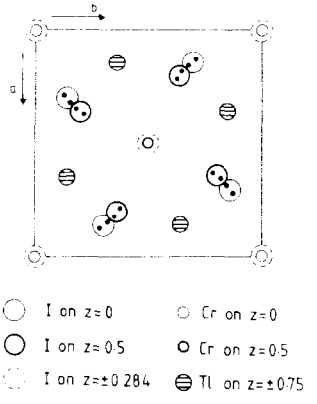

FIG. 3. A (0 0 1) projection of the structure of α-Tl_4CrI_6. The black dots represent the positions of the divided I(2) ion at 77 K.

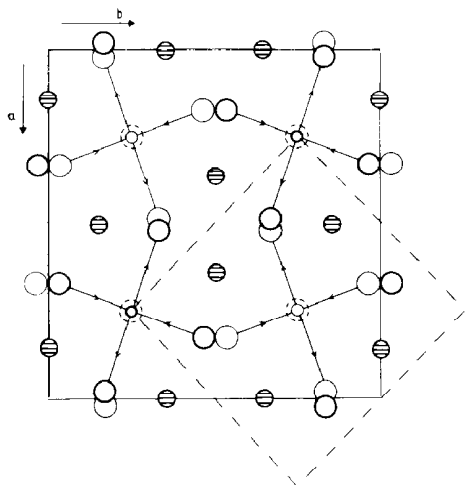

FIG. 4. A (0 0 1) projection of the structure of β-Tl_4CrI_6. The representation of the ions is given in Fig. 3. The dashed lines represent the axes of the unit cell of α-Tl_4CrI_6.

weakly ferromagnetic exchange interaction. J_4 has an exchange path via two empty orbitals and is predicted to be weakly antiferromagnetic. Further, J_1, J_2, and J_3 have exchange paths via two empty, two empty, and two half-filled d orbitals, respectively, and are expected to be antiferromagnetic.

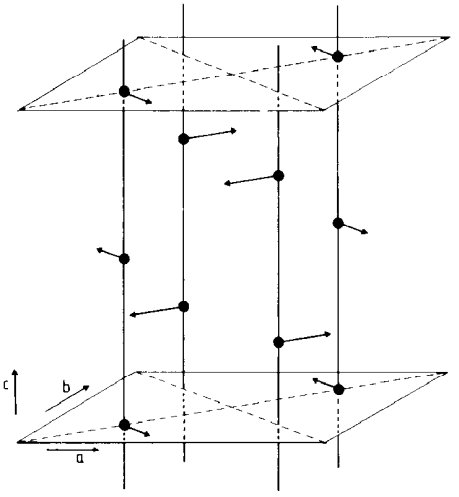

FIG. 5. The magnetic structure of β-Tl_4CrI_6. The magnetic moments make an angle of 41(9)° with the a axis.

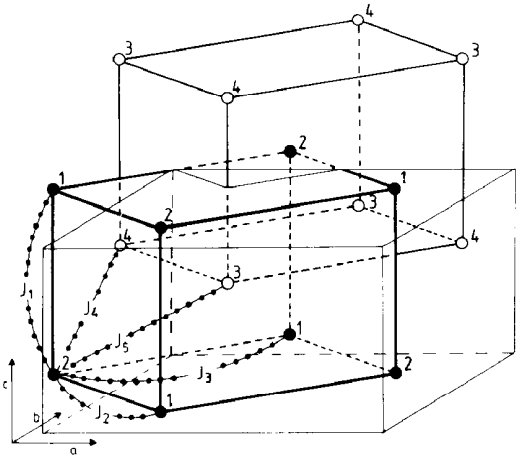

FIG. 6. The definition of the magnetic sublattices M_i (i = 1,4) and the exchange interactions J_j (j = 1,5).

Because of its geometry J_1 (a 180°–180° exchange path) is expected to be relatively strong.

For a more simple magnetic system, a body-centered tetragonal lattice where $J_2 = J_3$ and $J_4 = J_5$ the magnetic ordering phase diagram is calculated by Smart (*11*). The magnetic ions in α-Tl_4CrI_6 form such a lattice. Because of the special relations between J_1, J_2, and J_4 the three-dimensional phase diagram can be simplified to a two-dimensional β_1–β_2 phase diagram (see Fig. 7), where β_1, is $J_1/|J_4|$ and β_2 is $J_2/|J_4|$. For β-Tl_4CrI_6 the magnetic ordering phase diagram is five-dimensional. The β_1–β_2 phase diagram for $J_2 = J_3$ and $J_4 = -J_5$ is depicted in Fig. 8. When $J_4 = -J_5$ a C_c magnetic space lattice type is obtained instead of a spiral structure which occurs when $J_4 \neq -J_5$. With respect to the tetragonal system, the magnetic ordering type $A\,F_3$ is stable in a larger area due to $J_4 = -J_5$. With $J_2 = J_3$, a deviation from $J_4 = -J_5$ leads to a shift of the phase boundaries in the direction of those in Fig. 7. Using the magnetic ordering phase diagrams (Figs. 7 and 8), the magnetic structure of β-Tl_4CrI_6 suggests J_1, J_2, and J_3 to be antiferromagnetic and J_1 to be relatively strong. This is

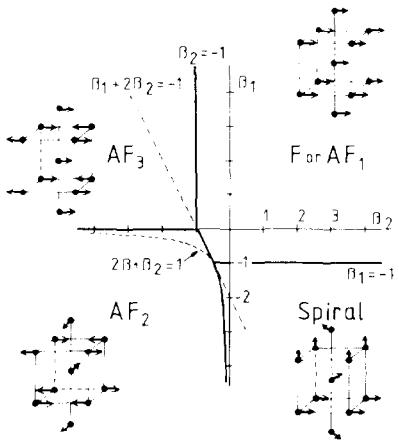

FIG. 7. Magnetic ordering phase diagram for a body-centered tetragonal lattice of the magnetic ions as for instance for α-Tl_4CrI_6. The spin orientations given in the figure for F or A F_1 and for Spiral are obtained with $J_4 + J_5$ being ferromagnetic.

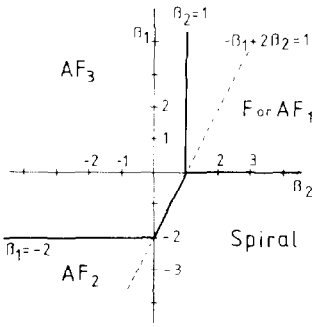

FIG. 8. Magnetic ordering phase diagram for β-Tl_4CrI_6 with $J_2 = J_3$ and $J_4 = -J_5$.

in accordance with the predictions for these exchange interactions discussed above.

It is worth noting that whereas In_4CrI_6 (*12*) ($\theta = -8(2)$ K, μ(eff) = 4.6(2) μ_B, T_c = 2.9(2) K) shows a deviation from a linear temperature dependence at about 6 K, similar to Tl_4CrI_6, the almost isostructural (tetragonal, without a Jahn–Teller deformation) compounds Tl_4MnI_6 (θ = 5(1) K, μ(eff) = 5.8(1) μ_B) and Tl_4FeI_6 (θ = 17(2) K, μ(eff) = 5.8(1) μ_B) (*12*) show no deviation from the linear temperature dependence down to 2 K. For a cubic system, more advanced calculations (*11*) predict a drop in the transition temperature when a phase boundary is approached. This might be the case for Tl_4MnI_6 and Tl_4FeI_6.

Acknowledgments

The author wishes to thank Dr. L. J. de Jongh, Dr. D. J. W. IJdo, and Dr. R. A. G. de Graaff for helpful discussions and a critical reading of the manuscript, and Mr. J. Strang of the Energieonderzoek Centrum Nederland for performing the neutron diffraction experiments.

References

1. H. W. ZANDBERGEN, *Acta Crystallogr. Sect. B* **35**, 2852 (1979).
2. N. JOUINI, L. GUEN, R. MARCHAND, AND M. TOURNOUX, *Ann. Chim. Fr.* **5**, 493 (1980).
3. G. E. BACON, Compilation, Neutron Diffraction Newsletter, ed. W. B. Yelon, May 1977.
4. R. E. WATSON AND A. J. FREEMAN, *Acta Crystallogr.* **14**, 27 (1961).
5. H. M. RIETVELD, *J. Appl. Cryst.* **2**, 65 (1969).
6. H. T. WITTEVEEN, Thesis, Leiden, The Netherlands (1973).
7. W. OPECHOWSKI AND R. GUCCIONE, *in* "Magnetism," Vol. IIA, Academic Press, New York (1963).
8. W. J. CRAMA AND H. W. ZANDBERGEN, *Acta Crystallogr.*, in press.
9. P. KOEHLER, Thesis, Marburg/Lahn, West Germany (1976).
10. J. B. GOODENOUGH, "Magnetism and the Chemical Bond," Interscience, New York (1963).
11. J. S. SMART, "Effective Field Theories of Magnetism," Saunders, Philadelphia (1966).
12. H. W. ZANDBERGEN, Thesis, Leiden, The Netherlands (1981).